**Photosensitizers for photodynamic therapy: Structure-activity analysis of cyanine dyes through design of experiments**

# Photosensitizers for photodynamic therapy: Structure-activity analysis of cyanine dyes through Design of Experiments

C. Pontremoli[a,†], G. Chinigò[b,†], S. Galliano[c], M.J. Moran Plata[a,§], D.M. Dereje[a,d], E. Sansone[b], A. Gilardino[b], C. Barolo[a], A. Fiorio Pla[b], S. Visentin[e], N. Barbero[a,*]

[a] University of Torino, Department of Chemistry, NIS Interdepartmental Centre and INSTM Reference Centre, Via Quarello 15a, 10135, Turin, Italy
[b] University of Torino, Department of Life Sciences and Systems Biology, Via Accademia Albertina 13, 10123 Turin, Italy
[c] University of Torino, Department of Agricultural, Forest and Food Sciences, Largo Paolo Braccini 2, 10095, Grugliasco (TO), Italy
[d] Department of Chemical Engineering, Bahir Dar Institute of Technology, Bahir Dar University, Polypeda 01, 0026 Bahir Dar, Ethiopia
[e] University of Torino, Department of Molecular Biotechnology and Health Science, via Quarello 15a, 10135, Turin, Italy.
[§] Present address: Donostia International Physics Center, Paseo Manuel de Lardizabal 4, 20018 Donostia, Spain.
* Corresponding author, nadia.barbero@unito.it
† These authors contributed equally to this work

## Highlights

- Pentamethine cyanines with different substituents have been synthesized for PDT
- CY-C4, Br-CY-C4, and I-CY-C4 showed fast ROS production
- DoE was applied to investigate CYs photoactivity and the structure-activity relationship
- CY-C4 and Br-CY-C4 revealed the greatest photoactive potential against MCF-7 cells
- COOH-CY-C4 did not show phototoxicity and has not been internalized by MCF-7 cells

## Abstract

In this work, a new series of pentamethine indolenine cyanine dyes has been designed and synthesised with the aim to investigate a structure-activity relationship on their photodynamic activity. The heteroaromatic indolenine ring has been differently functionalized (no substituents, bromine, iodine and carboxylic acid) to determine the effect of the substitution on the ROS production, cytotoxicity, photodynamic activity and cellular uptake. A statistical multivariate design such as the Design of Experiments (DoE) has been applied to evaluate which factor greatly affects the cyanine photoactive behavior, maximizing the information content, precision and accuracy in the results, while keeping the number of experiments low. All the synthesised dyes present low cytotoxicity in dark, but only some of them are able to promote phototoxic effect, upon irradiation, in MCF-7 cell lines, confirming a structure-activity relationship.

## Keywords

Photodynamic therapy; NIR Photosensitizer; Symmetrical Pentamethine Cyanines; Design of Experiments; Phototoxicity.

# 1. Introduction

Photodynamic therapy (PDT) is a minimal invasive [1–4] and high selective [1,2] technique for a wide range of applications, spanning from theragnostic [5,6], antimicrobial applications [7] to cancer therapies, representing a promising alternative to the traditional treatments. The main characters of PDT are the photosensitizer (PS), light with an appropriate energy to penetrate the tissue window [8,9], and molecular oxygen [10]. The PS, if excited by a non-thermal light (*i.e.* LED) at the appropriate excitation wavelength, reacts with oxygen, leading to the generation of reactive oxygen species (ROS), responsible for the oxidative damage and the cell death induced by necrosis and/or apoptosis [2,10].

Since the success of the therapy is strictly correlated to the photochemical and photophysical properties of the PS, the design of new PSs possessing high ROS generation ability and high selectivity for the target represents an essential step to improve the effectiveness of PDT. To date, one of the most significant drawbacks related to PDT is the lack of efficient clinically approved PSs and the request for novel molecules with ideal properties for their use in this therapeutic strategy is rapidly increasing. In fact, during the last decades, a great number of photosensitizers have been developed and some of them are currently clinically used in PDT, including porphyrins (Photofrin®) and chlorins. However, despite their efficacy, one of the major issues, along with the high skin photosensitivity, is their non-specificity and poor tissue penetration due to their light absorption in the ultraviolet–visible (UV–vis) range. To overcome these limitations, several efforts have been devoted to design and synthesize a new generation of PSs, with strong absorbance in the Near-Infrared Region (NIR), which induces higher light penetration, lower phototoxicity to normal tissues and thus an increased activity on the tumor regions. Among different NIR photosensitizers, polymethine dyes, i.e. squaraines and cyanines, have gained considerable attentions for wide application in various fields of science and technology (i.e PDT and imaging [8,11–13], protein detection [14–16], luminescence solar concentrator [17], dye-sensitized solar cells [18,19]). Compared to other classes of PSs such as phthalocyanines, porphyrins and their derivatives, the clinical application of cyanines in PDT is still limited, even if they can be considered promising PSs, thanks to their broad absorption spectral range with high extinction coefficients, high fluorescence quantum yield (QY), relatively high selectivity to tumor cells, low dark toxicity and side effects [13]. Cyanines can be synthesized with a high degree of chemical purity by following inexpensive and simple synthesis procedures. In addition, to increase the photochemical activity, the cancer cell selectivity and to avoid dark cytotoxicity and side effects, the cyanine's structure can also be tuned to obtain stable molecules showing the proper photophysical and photochemical properties, according to the desired applications [13,20,21]. Most of the cyanines proposed in literature as PSs are modifications of Indocyanine Green (ICG) to get more efficient PSs. Differently to ICG, all these Cy7 dyes are based on the indolenine ring instead of benzoindolenine one and most of them possess a stabilised bridge with a cyclohexene moiety, substituted by a chlorine atom [13]. Very few examples are reported on the use of penthamethine cyanines as PSs for PDT: Huang et al. [22] published three symmetric indolenine-based Cy5 where the central (meso) position of the bridge was substituted with different halogen groups. Recently, our research group synthesized a new series of NIR symmetrical penthametine cyanine dyes based on the benzoindolenine ring with different substituents and alkyl chain length in order to implement a structure-activity study and to evaluate the influence of the substitutions on the cellular uptake, ROS production and photodynamic activity [21]. To our surprise,

the presence or absence of the heavy atom was not highly affecting the PDT activity which seemed more influenced on the length of the alkyl chain probably due to the higher distance of the bromine from the central core. In this scenario, a deeper structure-activity relationship investigation based on indolenine-based Cy5 is needed.

Since the molecular design is an essential step in the development of new pharmaceutical products, given the large number of possibilities to modify the cyanine structure to get an efficient PSs, a large number of experiments will be needed to evaluate the photodynamic activity exerted by the different substitutions. In addition, the optimization of photodynamic treatment involves different parameters which could affect the therapy success, such as the dye concentration, the time of the PDT process as well as the time interval between photosensitizer administration and light irradiation, the fluence and the fluence rate, further increasing the time, the cost and the total number of experiments. To face this challenge, a statistical multivariate design such as the Design of Experiments (DoE) could be effectively applied. The DoE is a statistical approach, that allows to maximize the information content, precision and accuracy in the results, while keeping the number of experiments low. In fact, the DoE gives the possibility to plan and conduct experiments with deliberate alterations at input variables of a system, allowing the identification of the reasons for changes in final results [23]. By following this approach, the variables able to greatly influence a system can be evaluated and the input parameters can be defined to obtain answers closer to the desired results [24]. The DoE is a useful tool already applied in many academic and industrial fields and an appealing approach even in the context of drug discovery [25–27].

In this contribution, in order to investigate the structure-activity relationship, a new series of pentamethine cyanine dyes bearing different substituent groups (no substituent, Iodine, Bromine and Carboxylic group) on the indolenine ring has been synthesized, characterized and *in vitro* tested to evaluate their cyto- and phototoxicity and their cellular uptake. In order to run a low number of in *vitro* experiments and maximize the results, as well as to observe which variables mainly contribute to affect the cyanine activity, a DoE has been applied by using a two-level full factorial design. Light irradiation time, dye concentration and the time in cell culture after PDT treatment (DIC) have been selected as factors, while the absorbance, proportional to the cell viability after the irradiation, has been indicated as response. The modelling allowed to highlight the structure-activity relationship of the proposed cyanines, as well as to identify the more photoactive molecular structure (Figure 1).

## 2. Materials and methods

All the chemicals were purchased from Sigma Aldrich, Fluka, Merck or Riedel de Haen and were used without any further purification. 5-Carboxy-2,3,3-trimethyl-3H-indole (**1d**) was purchased from Intatrade Chemicals GmbH. 2,3,3-trimethyl-3H-indole (**1a**) and 5-carboxy-2,3,3-trimethyl-3H-indole (**1d**) are commercially available while 5-bromo-2,3,3-trimethyl-3H-indole (**1b**) and 5-iodo-2,3,3-trimethyl-3H-indole (**1c**) were prepared as previously described [8].

All microwave reactions were performed in single-mode Biotage Initiator 2.5. TLCs were performed on silica gel 60 F254 plates. ESI-MS spectra were recorded using a LTQ Orbitrap (Thermo Scientific) spectrometer, with electrospray interface and ion trap as mass analyzer. The flow injection effluent was delivered into the ion source using nitrogen as sheath and auxiliary gas. $^{1}$H NMR (600 MHz) and

$^{13}$C NMR (151 MHz) spectra were recorded on a Bruker Avance 600 NMR in $CDCl_3$, MeOD-$d^4$ or DMSO-$d^6$.

## 2.1 Synthetic procedures

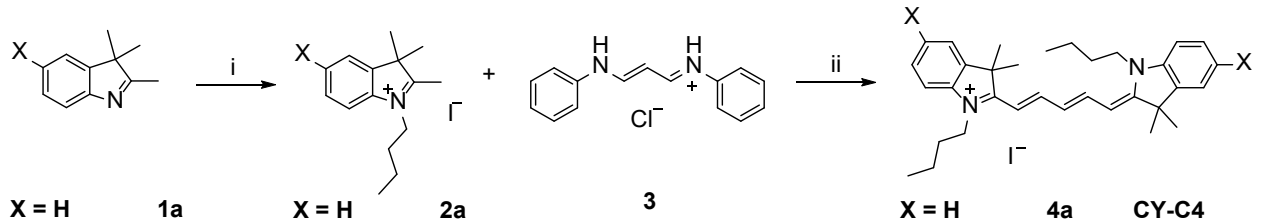


***Scheme 1.*** *Synthesis of symmetrical cyanine dyes. Experimental conditions: (i) acetonitrile, 1-iodobutane, MW, 15-30 min, 155 °C; (ii) sodium acetate, acetic anhydride, MW, 20-30 min, 130 °C.*

### 2.1.1 General quaternization synthesis of indolenines

2,3,3-trimethyl-3H-indoles (**1a-1d**), iodobutane (4 equivalents), and acetonitrile were introduced in a reaction vial, sealed with a crimp cap and heated in microwave system at 155 °C for 15-30 min. The solvent was removed and the solid was washed three times with diethyl ether and filtered to get the desired compound (**2a-2d**).

*1-butyl-2,3,3-trimethyl-3H-indol-1-ium iodide (**2a**)*. 2,3,3-trimethyl-3H-indole (**1a**) (750 mg, 4.7 mmol), iodobutane (2,14 mL, 18.8 mmol) and acetonitrile (2 mL) were reacted as described in the general procedure at 155 °C for 15 min, giving the title compound as a brownish solid (1.23 g, yield=76%).

$^1$H NMR (600 MHz, DMSO-$d^6$) δ 7.99 – 7.95 (m, 1H), 7.84 (dd, *J* = 5.9, 2.7 Hz, 1H), 7.62 (dd, *J* = 5.5, 2.8 Hz, 2H), 4.45 (t, *J* = 7.7 Hz, 2H), 2.84 (s, 3H), 1.82 (dd, *J* = 9.1, 6.4 Hz, 2H), 1.53 (s, 6H), 1.43 (dd, *J* = 15.4, 7.5 Hz, 2H), 0.94 (t, *J* = 7.4 Hz, 3H).

*5-bromo-1-butyl-2,3,3-trimethyl-3H-indol-1-ium iodide (**2b**).* 5-bromo-2,3,3-trimethyl-3H-indole (**1b**) (500 mg, 2.1 mmol), 1-iodobutane (0.7 mL, 6.3 mmol) and acetonitrile (2 mL) were reacted as described in the general procedure at 155 °C for 30 min, giving the title compound as a brownish solid (603 mg, 68 % yield).

$^1$H NMR (600 MHz, DMSO-$d^6$): δ = 8.20 (s, 1H), 7.97 (d, J = 8.0 Hz, 1H), 7.84 (d, J = 8.0 Hz, 1H), 4.45 (mt, J = 7.0 Hz, 2H), 2.85 (s, 3H), 1.87-1.72 (m, 2H), 1.55 (s, 6H), 1.47-1.36 (m, 2H), 0.92 (t, J = 7.5 Hz, 3H)

*5-iodo-1-butyl-2,3,3-trimethyl-3H-indol-1-ium iodide (**2c**).* 5-iodo-2,3,3-trimethyl-3H-indole (**1c**) (211 mg, 0.742 mmol), 1-iodobutane (0.44 mL, 1.5 mmol) and acetonitrile (2 mL) were reacted as described in the general procedure at 155 °C for 30 min, giving the title compound as a brownish solid (126 mg, 60% yield).

$^1$H NMR (600 MHz, Methanol-$d^4$) δ 8.19 (s, 1H), 8.01 (dd, 1H), 7.67 (d, *J* = 8.4 Hz, 1H), 4.48 (t, 2H), 4.10 (q, *J* = 7.1 Hz, 3H), 1.96 – 1.88 (m, 2H), 1.61 (s, 6H), 1.56 – 1.48 (m, 2H), 1.04 (t, *J* = 7.4 Hz, 3H).

*5-carboxy-1-butyl-2,3,3-trimethyl-3H-indol-1-ium iodide (**2d**).* 5-carboxy-2,3,3-trimethyl-3H-indole (**1d**) (2.50 g, 12.3 mmol), 1-iodobutane (5.6 mL, 49.2 mmol) and acetonitrile (10 mL) were reacted as described in the general procedure at 155 °C for 20 min, giving the title compound as pink powder (4.10 g, 86% yield).
$^1$H NMR (600 MHz, DMSO-d$^6$): δ = 8.39 (s, 1H), 8.14 (m, 2H), 4.49 (m, 2H), 2.92 (s, 3H), 1.83 (m, 2H), 1.58 (s, 6H), 1.46-1.40 (m, 2H), 0.93 (t, J = 7.5, 3H)

### 2.2.1 General synthesis of symmetrical cyanines

Compounds **2a-d** (2 equivalents), N-((1E,2E)-3-(phenylamino)allylidene) benzenaminium chloride (**3**) (1 equivalent), anhydrous sodium acetate (3 equivalents) and acetic anhydride were introduced in a microwave vial and heated at 130 °C for 15–30 min. The reaction mixture was poured in diethyl ether to precipitate a blue solid, which was washed with diethyl ether and filtered. The blue solid was dissolved in DCM leaving unreacted sodium acetate crystals on the filter funnel. The filtrate was evaporated under vacuum to obtain the cyanine dyes as a blue/brownish powder, except for COOH-CY-C4 where a RP column chromatography was needed.
*1-butyl-2-((1E,3E)-5-((Z)-1-butyl-3,3-dimethylindolin-2-ylidene)penta-1,3-dien-1-yl)-3,3-dimethyl-3H-indol-1-ium iodide* (**4a, CY-C4**). 1-butyl-2,3,3-trimethyl-3H-indol-1-ium iodide (**2a**) (686 mg, 2 mmol), N-((1E,2E)-3-(phenylamino)allylidene)benzenaminium chloride (**3**) (258.7 mg, 1 mmol), anhydrous sodium acetate (246 mg, 3 mmol) and acetic anhydride (15 mL) were introduced in a microwave vial and heated at 130 °C for 30 min. **4a** was obtained as a brownish powder (240 mg, yield=52%).
$^1$H NMR (600 MHz, $CDCl_3$) δ 8.23 (t, *J* = 13.0 Hz, 2H), 7.37 – 7.34 (m, 4H), 7.24 – 7.20 (m, 2H), 7.06 (d, J = 7.9 Hz, 2H), 6.83 (t, J = 12.4 Hz, 1H), 6.33 (d, J = 13.6 Hz, 2H), 4.06 (t, J = 7.6 Hz, 4H), 1.79 (s, 12H), 1.81 – 1.77 (m, 16H), 1.50 (m, 4H), 1.01 (t, J = 7.4 Hz, 6H) ppm.
$^{13}$C NMR (151 MHz, $CDCl_3$) δ 185.82, 173.21, 153.83, 142.24, 141.58, 128.66, 126.40, 125.22, 122.47, 110.61, 103.85, 49.60, 44.49, 29.63, 28.30, 20.44, 14.02. ppm.
HRMS (ESI) calcd for $[M-I]^+$ 467.3421 m/z, found 467.3429 m/z

*5-bromo-2-((1E,3E)-5-((Z)-5-bromo-1-butyl-3,3-dimethylindolin-2-ylidene)penta-1,3-dien-1-yl)-1-butyl-3,3-dimethyl-3H-indol-1-ium iodide* (**4b, Br-CY-C4**). 5-bromo-1-butyl-2,3,3-trimethyl-3H-indol-1-ium iodide (**2b**) (130 mg, 0.3 mmol), N-((1E,2E)-3-(phenylamino)allylidene)benzenaminium chloride (**3**) (38 mg, 0.15 mmol), anhydrous sodium acetate (37 mg, 0.45 mmol) and acetic anhydride (15 mL) were introduced in a microwave vial and heated at 130 °C for 30 min. **4b** was obtained as a brownish powder (80 mg, yield=43%).
$^1$H NMR (600 MHz, $CDCl_3$) δ 8.18 (t, J = 13.0 Hz, 2H), 7.47 (dd, J = 8.39, 1.90 Hz, 2H), 7.45 (d, J = 1.9, 2H), 6.94 (d, *J* = 8.4 Hz, 3H), 6.38 (d, *J* = 13.6 Hz, 2H), 4.06 (t, *J* = 7.6 Hz, 4H), 1.77 (s, 12H), 1.75 (m, 4H), 1.49 – 1.46 (m, 4H), 0.99 (t, *J* = 7.3 Hz, 6H) ppm
$^{13}$C NMR (151 MHz, $CDCl_3$) δ 172.59, 154.13, 143.50, 141.40, 131.66, 127.63, 125.90, 118.29, 111.96, 104.62, 49.60, 44.79, 29.61, 28.31, 20.47, 14.07, 1.16 ppm.
HRMS (ESI) calcd for $[M-I]^+$ 623.1631 m/z, found 623.1640 m/z

*1-butyl-2-((1E,3E)-5-((Z)-1-butyl-5-iodo-3,3-dimethylindolin-2-ylidene)penta-1,3-dien-1-yl)-5-iodo-3,3-dimethyl-3H-indol-1-ium* (**4c, I-CY-C4**). 5-iodo-1-butyl-2,3,3-trimethyl-3H-indol-1-ium iodide (**2c**) (250 mg, 0.533 mmol), N-((1E,2E)-3-(phenylamino)allylidene)benzenaminium chloride (**3**) (69 mg, 0.266 mmol), anhydrous sodium acetate (65 mg, 0.799 mmol) and acetic anhydride (3

mL) were introduced in a microwave vial and heated at 130 °C for 20 min. **4c** was obtained as a brownish powder (100 mg, yield=40%).
$^{1}$H NMR (600 MHz, DMSO-d$^{6}$) δ 8.34 (t, *J* = 13.1 Hz, 2H), 8.05 (s, 2H), 7.73 (d, *J* = 8.2 Hz, 2H), 7.23 (d, *J* = 8.3 Hz, 2H), 6.60 (t, *J* = 12.3 Hz, 1H), 6.30 (d, *J* = 13.7 Hz, 2H), 4.06 (t, *J* = 7.4 Hz, 4H), 1.67 (s, 12H), 1.63 (q, *J* = 7.6 Hz, 4H), 1.36 (q, *J* = 7.6 Hz, 4H), 0.91 (t, *J* = 7.4 Hz, 6H) ppm.
$^{13}$C NMR (151 MHz, DMSO-$D_6$) δ 172.14, 154.40, 143.65, 141.90, 136.93, 131.26, 126.20, 113.36, 103.48, 89.01, 48.94, 43.30, 29.02, 26.94, 19.44, 13.76.
HRMS (ESI) calcd for [M-I]$^{+}$ 719.1354 m/z, found 719.1362 m/z

*1-butyl-2-((1E,3E)-5-((Z)-1-butyl-5-carboxy-3,3-dimethylindolin-2-ylidene)penta-1,3-dien-1-yl)-5-carboxy-3,3-dimethyl-3H-indol-1-ium iodide* (**4d, COOH-CY-C4**). 5-carboxy-1-butyl-2,3,3-trimethyl-3H-indol-1-ium iodide (**2d**) (355 mg, 0.867 mmol), N-((1E,2E)-3-(phenylamino)allylidene)benzenaminium chloride (**3**) (110 mg, 0.433 mmol), anhydrous sodium acetate (106 mg, 1.23 mmol) and acetic anhydride (7.5 mL) were introduced in a microwave vial and heated at 130 °C for 25 min. **4d** was obtained as a brownish powder after RP column chromatography ($H_2O$/MeOH) (60 mg, yield=20%).
$^{1}$H NMR (600 MHz, MeOD-d$^{4}$) δ 8.31 (t, *J* = 13.1 Hz, 2H), 8.06 (d, *J* = 7.7 Hz, 4H), 7.32 (d, *J* = 7.9 Hz, 2H), 6.68 (t, *J* = 12.4 Hz, 1H), 6.35 (d, *J* = 13.6 Hz, 2H), 4.12 (t, *J* = 7.3 Hz, 4H), 1.77 (dd, *J* = 16.2, 6.7 Hz, 4H), 1.73 (d, *J* = 1.9 Hz, 12H), 1.52 – 1.42 (m, 4H), 1.02 – 0.97 (m, 6H) ppm.
$^{13}$C NMR (151 MHz, MeOD-d$^{4}$) δ 175.50, 156.23, 146.55, 142.58, 132.09, 127.96, 124.64, 111.62, 105.56, 50.39, 49.85, 45.08, 30.63, 27.85, 21.17, 14.20 ppm.
HRMS (ESI) calcd for [M-I]$^{+}$ 555.3217 m/z, found 555.3230 m/z

## 2.2 Spectroscopic characterization of the symmetrical cyanines

### 2.2.1 UV–Vis spectroscopy

UV–Vis spectra were recorded on a Cary 300 Bio spectrophotometer (Varian, Santa Clara, CA, USA), by using solvents with different polarity in order to investigate the solvatochromic behavior of the symmetrical cyanines. UV–Vis measurements were carried out in the range of 500–800 nm and were recorded at room temperature. The powders were solubilized and analyzed after proper dilutions in acetone, absolute ethanol (EtOH), methanol (MeOH), dichloromethane (DCM), double distilled water (dd$H_2O$) and Dimethyl sulfoxide (DMSO).

### 2.2.2 Determination of molar extinction coefficient

In order to evaluate the molar extinction coefficient, a stock solution (0.5 mM) in DMSO of each dye was prepared and then different diluted solutions were obtained by taking proper aliquots of the stock solution. The diluted solutions (CY-C4 and COOH-CY-C4 = 0.5, 1.0, 2.0, 3.0, 4.0, 5.0 μM; I-CY-C4 and Br-CY-C4 = 0.5, 1.0, 2.0, 3.0, 4.0 μM) were measured by UV–Vis spectroscopy (Cary 300 Bio spectrophotometer, Varian, Santa Clara, CA, USA,) in the range of 500–800 nm using quartz cuvettes with a 1 cm pathway length.
The absorbance intensities of each solution at the $\lambda_{max}$ were plotted versus the sample concentration. A linear fit was applied to determine the molar extinction coefficient (ε) as the slope of the line. The analysis was performed in duplicate. The obtained data were considered acceptable when the difference between the measured log ε was less or equal to 0.02 in respect to their average.

### 2.2.3 Fluorescence spectroscopy

Fluorescence measurements were recorded using a HORIBA Jobin Yvon Fluorolog2 in the range of 630–750 nm. The excitation wavelength was different for every cyanine and was set at the cyanine shoulder previously recorded at the UV–Vis spectra. The excitation and emission slits were 5 nm and 5 nm, respectively. Diluted solutions with absorbance around or lower of 0.1 units were used to avoid the presence of aggregates. Fluorescence quantum yields were determined using the same instrument with Quanta-φ integrating sphere and De Mello method. The final result is an average of three independent measurements.

## 2.3 Evaluation of singlet oxygen generation ability

1,3-Diphenylisobenzofuran (DPBF) was used as scavenger molecules to evaluate singlet oxygen generation, by following the protocol previously described in the literature [8,28]. In fact, DPBF rapidly reacts with $^1O_2$ forming the colourless *o*-dibenzoylbenzene derivative. The $^1O_2$ scavenger activity can be monitored through a decrease in the electronic absorption band of DBPF at 415 nm.
Stock solutions of DPBF and dyes were prepared in DMSO. Each solution was then diluted in phosphate buffer (2 mM, pH 7.4) to obtain the final desired concentration (25 μM for DPBF and 5 μM for Cyanines), placed in a 1 cm quartz cell and irradiated in an aerated solar box (Solarbox 3000e, 250 W xenon lamp, CO.FO.ME.GRA) with a 250 W lamp at various time intervals. Light was filtered in an optical filter with a 515 nm cut-off, to avoid the DPBF degradation.
At predefined time points, absorption spectra were recorded on a Cary 300 Bio spectrophotometer instrument. The decrease in the DBPF absorption contribution at 415 nm was plotted as a function of the irradiation time.

## 2.4 Cell culture and cell viability assay

Human breast adenocarcinoma cell line (MCF-7, ECACC 86012803) was used to evaluate the cell viability before the light irradiation. MCF-7 were purchased from the European Collection of Authenticated Cell Cultures (ECACC, Salisbury, UK) and cultured in Dulbecco's Modified Eagle's Medium-high glucose (DMEM from Euroclone), complemented with 10% of Fetal Bovine Serum (Euroclone), 100 mg/mL PenStrep antibiotic (Sigma-Aldrich, Italy) and 5 mM L-glutamine (Sigma-Aldrich, Italy). All cell cultures were maintained at 37°C and 5% $CO_2$ in incubator, using Falcon™ plates as supports.
MCF-7 cells were seeded in 96-well plates at a density of $0.5 \cdot 10^4$ cells/well for cell viability assays. Once attached, MCF-7 were treated with different cyanine dyes concentrations (from 10 nM to 800 nM) and cell viability was assessed 24, 48 and 72 h after treatments using CellTiter 96 AQueous Non-Radioactive cell proliferation assay (Promega, USA) following manufacturer's instruction. For each condition, eight replicates were set up. Absorbance values recorded at 490 nm using a microplate reader (FilterMax F5, Multi-Mode Microplate Reader, Molecular Devices) were then analyzed with Excel software (Office, Microsoft) and GraphPad Prism 6 software (La Jolla, CA, USA) to assess statistical significance. At least three independent experiments were performed for each condition.

## 2.5 Photodynamic treatment and phototoxicity assay

Cyanines' photodynamic activity was evaluated plating MCF-7 cells in 96-well plates ($0.5 \cdot 10^4$ cells/well) and treating them O/N with 200 nM cyanine dyes. Cells were then irradiated with a light beam intensity of 8 mW/cm$^2$ for 15 minutes (Fluence = 7.2 J/cm$^2$) using a compact LED array-based illumination system specifically designed and produced by Cicci Research s.r.l (Italy). The proposed illumination system includes a RED-LED array (light source with excitation wavelength: 640 nm, and power: 8 mW/cm$^2$) composed of 96 LEDs arranged in 12 columns x 8 rows. 24 h, 48 h and 72 h after LED irradiation MTS assays were performed in order to evaluate the cell viability. MCF-7 treated with cyanines but not irradiated as well as MCF-7 irradiated but not treated with dyes were used as control for each experiment. For each condition eight replicates in at least three independent experiments were performed.

## 2.6 Design of Experiment

MODDE 13 Pro software (Sartorius, Germany) was used to model CY photoactivity reducing screening time and experimental resources. For this purpose, exposure time to the light beam (LB, min) $X_1$, dye concentration (Conc, nM) $X_2$, and incubation time in culture after irradiation (DIC, h) $X_3$ were selected as independent factors. The response (Y) was identified as the absorbance values correlated to cell viability.
A preliminary Design of Experiment has been performed on each cyanine to observe the influences of all experimental variables (factors) and their interaction on the response. We adopted a two-level full factorial design (FullFac) with center point. The two levels represent the limits (- and + in matrix term) of the factors: 0-200 nM for dye concentration; 24-72 h for DIC; 0-15 min for exposure time to the light beam. Given a process with *k* factors, where each is investigated at two levels, a full factorial design will consist of $2^k$ experiments, corresponding to all different combinations of factors set at their limits. Differently the center point corresponds to the combination of all factors set at their mean value (0 in matrix term). In this investigation, the design suggests performing only 8 different experiments and a center point for each CY, that are summerized in the experimental matrix reported in Table 1.

Three independent experiments, with 8 technical replicates each, were performed for each condition. Absorbance values were calculated as the average value from each group of replicates. These three averaged values were used in the DoE model. Moreover, experimental cell viability data used for the DoE were normalized to the control measured 24 h after light irradiation.
The absorbance Y was represented as a function of the three factors using a third-order interaction model described by the following general equation:

$$y = b_0 + b_1X_1 + b_2X_2 + b_3X_3 + b_{12}X_1X_2 + b_{13}X_1X_3 + b_{23}X_2X_3 + b_{123}X_1X_2X_3$$

with $b_i$ being the terms of the polynomial obtained from the fitting, and y the interpolated absorbance obtained from the model. As a consequence, with just 8 experiments and one for the central point, it is possible to estimate one constant term ($b_0$), three linear terms ($X_1$, $X_2$, $X_3$), three two-term interactions ($X_1X_2$, $X_1X_3$, $X_2X_3$) and the three-term interaction ($X_1X_2X_3$). By comparing the coefficients, it is possible to understand which factor most influences the response and whether there are significant interactions among the factors.

In the second part of the study, a more detailed and complex DoE, with same factors and response, has been adopted to properly model the photoactive behaviour of Br-CY-C4. A $2^k x 3^p$ Full Factorial Mixed design was selected with one factor at two-level (0-15 min for LB) and two factors at three-level (0, 100, 200 nM for dye concentration; 24, 48, 72 h for DIC). The selected design required a total of 19 experiments, comprising the previously performed 9 experiments (Table 1) and 10 new experiments (Table 2). Three independent experiments with 8 technical replicates each were performed for each experimental condition.

The selected DoE design improves the data modelling by implementing the quadratic terms ($b_{11}X_1^2, b_{22}X_2^2, b_{33}X_3^2$) in the model function. In fact, the latter allows to observe nonlinear trends of the factors, thus resulting in a more precise description of the experimental domain.
The robustness and predictive value of both DoE models were evaluated on the basis of the following model statistics parameters: the explained variation index ($R^2$) which indicates the goodness of model fit with a value between 0 and 1; the predict variation index ranging from 0 and 1 ($Q^2$) which evaluates the goodness of model predictions; the reproducibility (Rep.) which refers to the goodness of experiments repetition, *i.e.* variation of replicates.

## 2.7 Cellular uptake

To assess the intracellular uptake of the dyes, Calcein (Molecular probes®, Invitrogen) has been used to label and track the whole cellular volume in MCF-7 live cells. Briefly, MCF-7 cells were seeded in four Petri dishes ($12*10^4$ cells/dish), and 48 h after seeding cells were treated overnight with 200 nM of cyanines (CY-C4, Br-CY-C4, I-CY-C4, COOH-CY-C4). Then, cells were washed and incubated with Calcein (250 nM) for 30 min, washed twice with Hanks' Balanced Salt Solution (HBSS) to remove the excess probe and fixed in 4% paraformaldehyde (PAF) at 37°C for 4 min. The cells were then observed using a Leica TCS SP8 confocal system (Leica Microsystems, Germany) equipped with an HCX PL APO 63X/1.4 NA oil-immersion objective. To simultaneously detect the probes, cyanines were excited with a HeNe laser at 633 nm, whereas Calcein was excited with DPSS laser at 561 nm. Images were acquired on the three coordinates of the space (XYZ planes) with a resolution of 0.081 µm x 0.081 µm x 0.299 µm and were processed and analyzed with ImageJ software (Rasband, W.S., U.S. National Institutes of Health, Bethesda, MA). 3D images with Calcein allowed assessing whether dyes are within the cell or not.

## 2.8 Statistical analysis

Data are shown as mean ± SEM of one representative experiment out of three. Statistical analyses were performed using Graph-Pad Prism 6.0 software (La Jolla, CA, USA). Statistical significance between different conditions was determined by analysis of variance (Ordinary one-way ANOVA/Kruskal Wallis test) followed by *post-hoc* Dunn, Dunnett or Tuckey's multiple comparisons test. Differences with a p-values (p) < 0.05 were considered statistically significant and represented as follows *: $p < 0.05$; **: $p < 0.01$; ***: $p < 0.001$; ****: $p < 0.0001$.

# 3 RESULTS AND DISCUSSION

## 3.1 Synthesis of Cyanine dyes

The synthesis of symmetrical pentamethine cyanine dyes (**4a-4d**) involves the condensation of the quaternary heterocyclic salts (**2a-2d**), bearing an activated methyl group, with malonodialdehyde derivative (**3**). While 2,3,3-trimethyl-3H-indole (**1a**) and 2,3,3-trimethyl-3H-indole-5-carboxylic acid (**1d**) are commercially available, the 5-bromo-2,3,3-trimethyl-3H-indole (**1b**) and the 5-iodo-2,3,3-trimethyl-3H-indole (**1c**) were obtained exploiting the Fischer indole synthesis by reacting (3-bromophenyl)hydrazine or (3-iodophenyl)hydrazine, respectively, with 3-methylbutan-2-one in glacial acetic acid, as previously described [8,29]. The subsequent quaternization with 1-iodobutane of the four indolenine rings, performed under microwave irradiation, [29] led to an increased acidity of the methyl group which enabled the cyanine bridge formation (see first step in Scheme 1). The characterization of quaternarized salts of (**2a-d**) matched the previously reported in literature [8,29]. All the symmetrical cyanine dyes were synthesized in a one-step reaction under microwave heating by reacting two equivalents of quaternary heterocyclic salts with the malonoaldehyde bis(phenylimine) monohydrochloride (**3**) in presence of sodium acetate and acetic anhydride (see Scheme 1) [21]. The reaction mixture was then poured in diethyl ether to precipitate a solid, which was washed and filtered. This solid was then dissolved in DCM to remove unreacted sodium acetate crystals by filtration. Cyanine dyes were then obtained in moderate yields (from 20 to 52%) after the evaporation of DCM. For **COOH-CY-C4**, a further purification on RP chromatography was required to obtain a pure compound.

## 3.2 Spectroscopic characterization of the symmetrical cyanine dyes

The UV–vis absorption spectra recorded in DMSO (Figure 2) of all the Cyanine dyes show a narrow absorption band in the NIR, perfectly matching the phototherapeutic window, with absorption maxima between 650 nm and 662 nm and high molar extinction coefficients varying from 152,000 to 265,000 $M^{-1}cm^{-1}$ (log$\varepsilon$ between 5.18 and 5.42). The main absorption peak could be ascribed to the $\pi\rightarrow\pi^*$ HOMO–LUMO transitions, while the hypsochromic shoulder, typical for cyanine dyes [21,30,31], is associated to the HOMO-LUMO+1 transition. When excited on the hypsochromic shoulder, these cyanines show a luminescence spectrum with the emission maxima ranging from 670 to 691 nm.

The main photochemical properties obtained in different solvents are reported in Table 3. The presence of a different substituent on the indolenine ring (*i.e* -Br, -I, -COOH) seems to have a slight effect on the $\lambda_{max}$ suggesting that the electronic levels, involved in the $\pi$-$\pi^*$ transition, have similar energies. This behavior is in accordance with the data obtained by the authors reporting that the presence or absence of heavy atoms and the length of the alkyl chain did not lead to a large shift in the $\lambda_{max}$ on benzoindolenine phentamethine cyanines [21].
The solvatochromic effect on both the absorption and fluorescence spectra was also investigated as shown in Table 3. Although there is no linearity in the maximum absorption wavelength values of the dyes with the polarity of the solvents, it should be noted that, compared to MeOH, a 15 nm bathochromic shift has been induced by DCM suggesting a more polar ground state in comparison to

the excited one [21,32,33]. In addition, the use of protic or aprotic solvents seems not to induce any significant differences in both the absorption and emission peak maxima. The low Stokes shift value, around 20 nm for all solvents, could be associated to a moderate geometry change from the ground to the excited state. The fluorescence quantum yield was evaluated in DMSO and the obtained values, varying from 51 to 65% as expected for polymethine dyes, are reported in Table 3.

## 3.3Generation of singlet oxygen

A preliminary evaluation of the ability of this series of cyanines to generate reactive oxygen species (ROS) was carried out by using 1,3-diphenylisobenzofuran (DPBF) as a probe [8]. In fact, DPBF rapidly reacts with ROS generated by the PSs after the irradiation, forming the colorless o-dibenzoylbenzene derivative, resulting from the disappearance of DPBF's characteristic absorption band at 415 nm.

To evaluate the activity of the cyanines, the decrease in the DPBF absorption band at 415 nm, as a function of the irradiation time, has been compared to the values obtained by irradiating a standard, the efficient and well-known ROS generator Bengal Rose (BR). Thus, a solution of DPBF (25 μM), Bengal Rose as reference and cyanine dyes (5 μM) in PBS pH 7.4 and DMSO (1%) was mixed and irradiated in a filtered solar box to remove the wavelengths below 515 nm to avoid the DPBF degradation while DPBF consumption was monitored over time.

As shown in figure 3, all the cyanines except for the COOH-CY-C4 reveal a faster and higher ROS generation ability, compared to the BR. In particular, the halogenated I-CY-C4 and Br-CY-C4 are able to promote the complete decay of DPBF absorption within 2 minutes, while the same result was obtained in 8 min for the CY-C4 without any substituent. As already reported by the authors [8,21], the presence of both bromine and iodine may facilitate the singlet to triplet state intersystem crossing that is due to the well-known heavy atom effect.

## 3.4 CY *in vitro* cytotoxicity

To identify the maximum non-toxic concentration of CYs exploitable for PDT application, CY-C4, COOH-CY-C4, Br-CY-C4, and I-CY-C4 were tested on MCF-7 cells at different concentrations ranging from 10 to 800 nM. As shown in Figure 4, the unsubstituted (CY-C4) and the I-CY-C4 induce a significant decrease in cell viability already 24 h after the treatment starting from the concentration of 400 nM. Furthermore, the unsubstituted (CY-C4) and the I-CY-C4 showed the highest cytotoxicity compared to the other tested CYs, since 48 hours after treatment it weakly compromises cell viability even at a low concentration of 200 nM. On the other hand, Br-CY-C4 was cytotoxic just at 800 nM. In contrast, carboxyl-substituted cyanine (COOH-CY-C4) did not show any toxic effect at any of the investigated concentrations. Based on these results, 200 nM has been selected as the maximum non-toxic concentration of CYs to preliminary evaluate their photoactive behaviour.

## 3.5DoE and photoactivity modelling

Once verified that the light beam irradiation (fluence = 7.2 J/cm$^2$) does not affect cell viability (Figure S1), we used a Design of Experiment approach to investigate CYs photoactivity and deepen their structure-activity relationship. This approach allowed us to mathematically describe the photoactive

behavior of the different CYs within the experimental space, whit a limited number of experiments. As a preliminary screening, we investigated the experimental domain through a simple two-levels full factorial model with three variables. Therefore, we performed cell viability assays on MCF-7 based on the conditions defined by the experimental matrix reported in Table 1. Based on three independent experiments for each experimental point considered (Table 1), we obtained for each molecule a mathematical model of its photoactivity within the experimental domain. As reported in Figure S2, all the obtained models appear statistically robust, indeed both $R^2$ and $Q^2$ parameters are $\geq 0.7$ and very similar to each other indicating a strong statistical correlation.

Next, we evaluated the contribution induced by the factors and their interactions on photo-induced cytotoxicity. In Figure 5 and Table S1 the models' coefficients referring to each cyanine are reported. Coefficients' values are represented by green bars with confidence interval at 95%. A positive value means the absorbance will increase by increasing that factor, while it is the opposite with negative value. Coefficients with error bar crossing the x axis (0 value) are considered statistically non-significant. As expected, for all tested CYs the only positive contribution is due to the DIC parameter, which represents the major influencing factor for CY-C4 (0.51), Br-CY-C4 (0.55), and COOH-CY-C4 (0.78). This means that generally, considering the whole experimental domain, MCF-7 cells continue to proliferate during incubation time from 24 h to 72 h, independently from the initial treatment. However, by comparing the values of DIC coefficients between cyanines, it is possible to deduce some useful information on their cytotoxicity. Indeed, the greatest contribution of DIC on cell viability is observed in the case of COOH-CY-C4, which does not induce any cytotoxicity, confirming the *in vitro* results reported in Fig 4. On the contrary, I-CY-C4 show the lowest DIC value (0.31), while the concentration factor proved to be the main actor in influencing cell viability with the highest negative value (-0.56). Both coefficients clearly confirm the higher cytotoxicity associated with the iodine-substituted cyanine compared to bromine and unsubstituted derivatives. Furthermore, light beam exposure promotes a significant negative effect on cell viability after treatment with Br-CY-C4 (-0.47), CY-C4 (-0.34), and I-CY-C4 (-0.20), but not with COOH-CY-C4 (-0.07). These results are in good agreement with those obtained monitoring *in vitro* ROS production, confirming that among all the evaluated cyanines, the carboxyl-substituted is not photoactive. The same trend can be observed for the linear interaction LB*Conc. Being significantly related to both light exposure and dye concentration, LB*Conc coefficient can be considered a figure of merit to evaluate the photoactive behaviour of all the investigated cyanines. Based on the model predictions, Br-CY-C4 (-0.41) and CY-C4 (-0.26) revealed the greatest photoactive potential, as representatively shown by the experimental results reported in Figure 6.

After these preliminary evaluations, along with the cytotoxic assay in dark condition, Br-CY-C4 has been identified as the most suitable dye for PDT application among the different cyanines. Thus, we decided to further investigate its photoactive behaviour by performing a more detailed and predictive DoE based on a Full Factorial Mixed design. This design allows to improve the model function in describing the whole experimental domain, hence, to properly map the cell viability in function of all factor's variations. In addition to the previously performed experiments, 10 further experimental points have been tested with the same procedure. The data analysis reported in Fig 7A shows a more

robust model with improved predictive ability (increased $R^2$ and $Q^2$) compared to the simpler design previously performed on Br-CY-C4.

The significant coefficients of the model function are summarized in Fig 7B and 7C. Differently from the first model, this model function shows, together with three linear terms and two interactions, also the quadratic term LB*LB. This positive term means that the negative effect of light beam exposure on cell viability is more evident at shorter times while tends to decrease at longer times. In other words, the PDT effect of Br-CY-C4 is already expressed after few minutes of irradiation, indicating a rapid photo-induced cytotoxicity. Moreover, this behaviour, together with all the effects due to factors variation, can be clearly observed on cell viability through the Isoresponse contour Plot (Fig. 8). The absorbance rapidly decreases by increasing light exposure and dye concentration, thus confirming the strong photo-induced cytotoxicity, while it increases over the incubation time indicating the absence of cytotoxicity. In light of these results, Br-CY-C4 confirms to be a promising candidate to be used as photosensitizer in photodynamic therapy.

### 3.6 Intracellular uptake

Finally, the internalization of the cyanines within the cells was assessed by performing confocal laser scan microscopy experiments on MCF-7 cells treated O/N with 200 nM of the dyes. The whole cellular volume was labelled using Calcein (red signals in Fig. 9) and images were acquired on the three coordinates of the space (XYZ), allowing to reconstruct the 3D cellular volume and therefore to check whether dyes (green signals in Fig. 9) were included within the cellular volume or not. As shown in figure 9, CY-C4, Br-CY-C4, and I-CY-C4 are clearly internalized by MCF-7 after O/N incubation as shown by the good co-localization (in yellow) between the fluorescent signal of the dye (in green; $\lambda_{ex}$= 633 nm) and Calcein (in red; $\lambda_{ex}$= 561 nm). The intracellular localization of CY-C4, Br-CY-C4, and I-CY-C4 was further confirmed by the 3D reconstruction of the cell volume which reveals the probe signal within the calcein-labelled cell volume (orthogonal view in Fig. 9). In agreement with previous results obtained on another series of pentamethine derivatives [34], cyanines dyes homogeneously stains the cytoplasm producing a diffuse and delocalized fluorescent signal on the entire cell volume. By contrast, COOH-CY-C4 has not been internalized by the cells as revealed by the lack of green fluorescent signals in the cells treated with 200 nM of COOH-CY-C4 (Fig. 9). These results support the hypothesis that the presence of a carboxyl group as a substituent in the indolenine ring not only affects the intersystem crossing process by preventing the production of ROS *in vitro* (Fig. 3) but it also hinders the cellular dye uptake, resulting in an overall lack of photodynamic activity of the molecule.

## 4 Conclusions

A structure-activity relationship study has been conducted on a new series of symmetrical pentamethine cyanine dyes showing absorption maxima in the range of 640 and 670 nm, matching the phototherapeutic window. The indolenine ring has been functionalized with different substituent

groups (no substituent, iodine, bromine and carboxylic group) to understand the influence of the substitution on ROS generation ability, cyto- and phototoxicity and their cellular uptake.
The non-substituted cyanine (CY-C4), iodine- and bromine-cyanines (I-CY-C4 and Br-CY-C4 respectively) showed a good ROS generation *in vitro*, a good cellular uptake and no cytotoxicity in the dark on MCF-7 cells up to a concentration of 200 nM. On the other hand, the COOH-CY5 showed a very slow and weak ROS production *in vitro* and a negligible cellular uptake. In order to minimize the number of *in vitro* experiments and maximize the results, a DoE has been applied by using a two-level full factorial design. The modelling allowed to highlight the structure-activity relationship of the proposed cyanines, as well as to identify the more photoactive molecular structure in the tested experimental conditions. In fact, DoE confirmed that COOH-CY-C4 is not photoactive, while CY-C4, I-CY-C4 and Br-CY-C4 showed light-induced cytotoxicity. A trend in the phototoxicity has been highlighted by the DoE: Br-CY-C4 > CY-C4 > I-CY-C4. Our data clearly suggest that the influence of the heavy atom is not always as remarkable as reported in the literature, confirming our previous results on benzoindolenine CY5 [21]. However, among these three cyanines, Br-CY-C4 resulted the more promising one, showing the higher increase in cell toxicity after irradiation. Therefore, a deepen DoE investigation has been adopted to analyse Br-CY-C4, which further highlighted the fast decreasing in cell viability by increasing light exposure and dye concentration as well as the cell viability increase over the incubation time indicating the absence of cytotoxicity.
This study pointed out the applicability of the DoE as a potential useful tool in the design and analysis of new photosensitizers in PDT. Further investigations are needed to confirm the therapeutical potential of pentamethine cyanines as photosensitizers for cancer treatment and to identify the presence of other relevant parameters able to affect the overall cyto- and phototoxicity of indolenine-based cyanines and to disclose the optimal modalities to maximize the response in term of phototoxicity.

# Author contributions

**C. Pontremoli**: Data curation; Formal analysis; Investigation; Methodology; Writing - original draft

**G. Chinigò**: Data curation; Formal analysis; Investigation; Methodology; Writing - original draft

**S. Galliano**: Data curation; Formal analysis

**M.J. Moran Plata**: Investigation; Methodology

**D.M. Dereje**: Data curation; Formal analysis

**E. Sansone**: Investigation; Methodology

**A. Gilardino**: Data curation; Formal analysis

**C. Barolo**: Supervision; Writing - review & editing

**A. Fiorio Pla**: Conceptualization; Supervision; Writing - review & editing

**S. Visentin**: Supervision; Writing - review & editing

**N. Barbero**: Conceptualization; Funding acquisition; Project administration; Supervision; Writing - review & editing

# Funding

This work was supported by the University of Torino (Ricerca Locale ex-60%, Linea A, Bando 2020), by the Fondazione CRT (II tornata 2019 RF.2019.2260).

# Acknowledgements

The authors are grateful to Vittoria Mitrugno for her contribution in the intracellular uptake study.


# 5 References


1. Lan, M.; Zhao, S.; Liu, W.; Lee, C.-S.; Zhang, W.; Wang, P. Photosensitizers for Photodynamic Therapy. *Adv. Healthc. Mater.* **2019**, *8*, doi:10.1002/adhm.201900132.
2. Li, L.; Huh, K. M. Polymeric nanocarrier systems for photodynamic therapy. *Biomater. Res.* **2014**, *18*, 1–14, doi:10.1186/2055-7124-18-19.
3. Ruan, Z.; Zhao, Y.; Yuan, P.; Liu, L.; Wang, Y.; Yan, L. PEG conjugated BODIPY-Br<inf>2</inf> as macro-photosensitizer for efficient imaging-guided photodynamic therapy. *J. Mater. Chem. B* **2018**, *6*, 753–762, doi:10.1039/c7tb02924a.
4. Zou, J.; Yin, Z.; Wang, P.; Chen, D.; Shao, J.; Zhang, Q.; Sun, L.; Huang, W.; Dong, X. Photosensitizer synergistic effects: D-A-D structured organic molecule with enhanced fluorescence and singlet oxygen quantum yield for photodynamic therapy. *Chem. Sci.* **2018**, *9*, 2188–2194, doi:10.1039/c7sc04694d.
5. Choi, J.; Kim, S. Y. Photothermally enhanced photodynamic therapy based on glutathione-responsive pheophorbide a-conjugated gold nanorod formulations for cancer theranostic applications. *J. Ind. Eng. Chem.* **2020**, doi:10.1016/j.jiec.2020.01.018.
6. Wu, J.; Sha, J.; Zhang, C.; Liu, W.; Zheng, X.; Wang, P. Recent advances in theranostic agents based on natural products for photodynamic and sonodynamic therapy. *View* **2020**, doi:10.1002/viw.20200090.
7. Pérez-Laguna, V.; Gilaberte, Y.; Millán-Lou, M. I.; Agut, M.; Nonell, S.; Rezusta, A.; Hamblin, M. R. A combination of photodynamic therapy and antimicrobial compounds to treat skin and mucosal infections: A systematic review. *Photochem. Photobiol. Sci.* **2019**, *18*, 1020–1029, doi:10.1039/c8pp00534f.
8. Serpe, L.; Ellena, S.; Barbero, N.; Foglietta, F.; Prandini, F.; Gallo, M. P.; Levi, R.; Barolo, C.; Canaparo, R.; Visentin, S. Squaraines bearing halogenated moieties as anticancer photosensitizers: Synthesis, characterization and biological evaluation. *Eur. J. Med. Chem.* **2016**, *113*, 187–197, doi:10.1016/j.ejmech.2016.02.035.
9. Felsher, D. W. Cancer revoked: Oncogenes as therapeutic targets. *Nat. Rev. Cancer* **2003**, *3*, 375–380, doi:10.1038/nrc1070.
10. Alejandro, V. C.; Mónica, F. P.; Xelha, A. P.; Mario, R.; Gabriel, R. O.; Norberto, F.; Eva, R. G. Brominated BODIPYs as potential photosensitizers for photodynamic therapy using a low irradiance excitation. *Polyhedron* **2020**, *176*, doi:10.1016/j.poly.2019.114207.
11. Xia, G.; Wang, H. Squaraine dyes: The hierarchical synthesis and its application in optical detection. *J. Photochem. Photobiol. C Photochem. Rev.* **2017**, *31*, 84–113, doi:10.1016/j.jphotochemrev.2017.03.001.
12. Magalhães, Á. F.; Graça, V. C.; Calhelha, R. C.; Ferreira, I. C. F. R.; Santos, P. F. Bioorganic & Medicinal Chemistry Letters Aminosquaraines as potential photodynamic agents : Synthesis and evaluation of in vitro cytotoxicity. **2017**, *27*, 4467–4470, doi:10.1016/j.bmcl.2017.08.004.
13. Dereje, D. M.; Pontremoli, C.; Moran Plata, M. J.; Visentin, S.; Barbero, N. Polymethine dyes for PDT: recent advances and perspectives to drive future applications. *Photochem. Photobiol. Sci.* **2022**, doi:10.1007/s43630-022-00175-6.

14. Butnarasu, C.; Barbero, N.; Barolo, C.; Visentin, S. Interaction of squaraine dyes with proteins: Looking for more efficient fluorescent turn-on probes. *Dye. Pigment.* **2021**, *184*, 108873, doi:10.1016/j.dyepig.2020.108873.
15. Butnarasu, C.; Barbero, N.; Barolo, C.; Visentin, S. Squaraine dyes as fluorescent turn-on sensors for the detection of porcine gastric mucin: A spectroscopic and kinetic study. *J. Photochem. Photobiol. B Biol.* **2020**, *205*, 111838, doi:10.1016/j.jphotobiol.2020.111838.
16. Butnarasu, C.; Pontremoli, C.; Barbero, N.; Visentin, S.; Jesus, M.; Plata, M. Special Issue Research Article Squaraine Dyes as Fluorescent Turn-on Probes for Mucins : A Step Toward Selectivity †. **2022**, doi:10.1111/php.13722.
17. Yang, C.; Sheng, W.; Moemeni, M.; Bates, M.; Herrera, C. K.; Borhan, B.; Lunt, R. R. Ultraviolet and Near-Infrared Dual-Band Selective-Harvesting Transparent Luminescent Solar Concentrators. *Adv. Energy Mater.* **2021**, *11*, doi:10.1002/aenm.202003581.
18. He, J.; Jo, Y. J.; Sun, X.; Qiao, W.; Ok, J.; Kim, T. il; Li, Z. Squaraine Dyes for Photovoltaic and Biomedical Applications. *Adv. Funct. Mater.* **2021**, *31*, 1–35, doi:10.1002/adfm.202008201.
19. Saccone, D.; Galliano, S.; Barbero, N.; Quagliotto, P.; Viscardi, G.; Barolo, C. Polymethine Dyes in Hybrid Photovoltaics: Structure-Properties Relationships. *European J. Org. Chem.* **2016**, *2016*, 2244–2259, doi:10.1002/ejoc.201501598.
20. Lange, N.; Szlasa, W.; Saczko, J.; Chwiłkowska, A. Potential of cyanine derived dyes in photodynamic therapy. *Pharmaceutics* **2021**, *13*, 1–17, doi:10.3390/pharmaceutics13060818.
21. Ciubini, B.; Visentin, S.; Serpe, L.; Canaparo, R.; Fin, A.; Barbero, N. Design and synthesis of symmetrical pentamethine cyanine dyes as NIR photosensitizers for PDT. *Dye. Pigment.* **2019**, *160*, 806–813, doi:10.1016/j.dyepig.2018.09.009.
22. Huang, H.; Long, S.; Li, M.; Gao, F.; Du, J.; Fan, J.; Peng, X. Bromo-pentamethine as mitochondria-targeted photosensitizers for cancer cell apoptosis with high efficiency. *Dye. Pigment.* **2018**, *149*, 633–638, doi:10.1016/j.dyepig.2017.11.010.
23. Junqueira, M. V.; Borghi-Pangoni, F. B.; Ferreira, S. B. S.; Rabello, B. R.; Hioka, N.; Bruschi, M. L. Functional Polymeric Systems as Delivery Vehicles for Methylene Blue in Photodynamic Therapy. *Langmuir* **2016**, *32*, 19–27, doi:10.1021/acs.langmuir.5b02039.
24. Montgomery, D. C. *Dosing and Analysis of Experiments*; 8th editio.; Wiley: Danvers, MA, 2013;
25. Fukuda, I. M.; Pinto, C. F. F.; Moreira, C. D. S.; Saviano, A. M.; Lourenço, F. R. Design of experiments (DoE) applied to pharmaceutical and analytical quality by design (QbD). *Brazilian J. Pharm. Sci.* **2018**, *54*, 1–16, doi:10.1590/s2175-97902018000001006.
26. Rosso, F.; Rizzetto, A.; Airi, A.; Khoma, K.; Signorile, M.; Crocellà, V.; Bordiga, S.; Galliano, S.; Barolo, C.; Alladio, E.; Bonino, F. Rationalization of TS-1 synthesis through the design of experiments. *Inorg. Chem. Front.* **2022**, *9*, 3372–3383, doi:10.1039/d2qi00643j.
27. Galliano, S.; Bella, F.; Bonomo, M.; Viscardi, G.; Gerbaldi, C.; Boschloo, G.; Barolo, C. Hydrogel electrolytes based on xanthan gum: Green route towards stable dye-sensitized solar cells. *Nanomaterials* **2020**, *10*, 1–19, doi:10.3390/nano10081585.
28. Miletto, I.; Fraccarollo, A.; Barbero, N.; Barolo, C.; Cossi, M.; Marchese, L.; Gianotti, E. Mesoporous silica nanoparticles incorporating squaraine-based photosensitizers: A combined experimental and computational approach. *Dalt. Trans.* **2018**, *47*, 3038–3046, doi:10.1039/c7dt03735j.
29. Barbero, N.; Magistris, C.; Park, J.; Saccone, D.; Quagliotto, P.; Buscaino, R.; Medana, C.; Barolo, C.; Viscardi, G. Microwave-Assisted Synthesis of Near-Infrared Fluorescent Indole-Based Squaraines. *Org. Lett.* **2015**, *17*, 3306–3309, doi:10.1021/acs.orglett.5b01453.
30. Park, J.; Barbero, N.; Yoon, J.; Dell'Orto, E.; Galliano, S.; Borrelli, R.; Yum, J.-H.; Di Censo, D.; Grätzel, M.; Nazeeruddin, M. K.; Barolo, C.; Viscardi, G. Panchromatic symmetrical squaraines: a step forward in the molecular engineering of low cost blue-greenish sensitizers for dye-sensitized solar cells. *Phys. Chem. Chem. Phys.* **2014**, *16*, 24173–24177,

doi:10.1039/C4CP04345F.
31. Alberto, G.; Barbero, N.; Divieto, C.; Rebba, E.; Sassi, M. P.; Viscardi, G.; Martra, G. Solid silica nanoparticles as carriers of fluorescent squaraine dyes in aqueous media: Toward a molecular engineering approach. *Colloids Surfaces A Physicochem. Eng. Asp.* **2019**, *568*, 123–130, doi:10.1016/j.colsurfa.2019.01.052.
32. Galliano, S.; Novelli, V.; Barbero, N.; Smarra, A.; Viscardi, G.; Borrelli, R.; Sauvage, F.; Barolo, C. Dicyanovinyl and Cyano-Ester Benzoindolenine Squaraine Dyes: The Effect of the Central Functionalization on Dye-Sensitized Solar Cell Performance. *Energies* **2016**, *9*, 486, doi:10.3390/en9070486.
33. Magistris, C.; Martiniani, S.; Barbero, N.; Park, J.; Benzi, C.; Anderson, A.; Law, C.; Barolo, C.; O'Regan, B. Near-infrared absorbing squaraine dye with extended π conjugation for dye-sensitized solar cells. *Renew. Energy* **2013**, *60*, 672–678, doi:10.1016/j.renene.2013.06.018.
34. Chinigò, G.; Gonzalez-Paredes, A.; Gilardino, A.; Barbero, N.; Barolo, C.; Gasco, P.; Fiorio Pla, A.; Visentin, S. Polymethine dyes-loaded solid lipid nanoparticles (SLN) as promising photosensitizers for biomedical applications. *Spectrochim. Acta Part A Mol. Biomol. Spectrosc.* **2022**, *271*, 120909, doi:10.1016/j.saa.2022.120909.

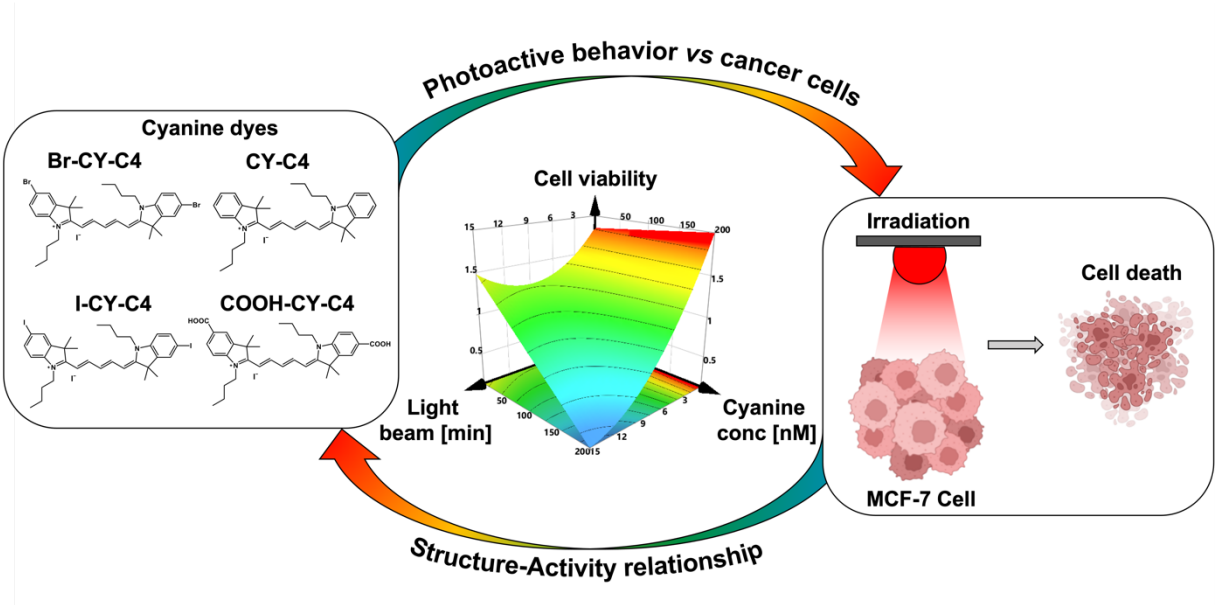


***Figure 1.*** *Schematic illustration of the aim of the work. The DoE was applied to investigate CYs photoactivity and the structure-activity relationship.*

***Table 1****. Experimental conditions of the DoE screening design.*

| *LB (min)* | *Conc (nM)* | *DIC (h)* |
|---|---|---|
| 0 | 0 | 24 |
| 15 | 0 | 24 |
| 0 | 200 | 24 |
| 15 | 200 | 24 |
| 0 | 0 | 72 |
| 15 | 0 | 72 |
| 0 | 200 | 72 |
| 15 | 200 | 72 |
| 7,5 | 100 | 48 |

***Table 2**. Additional experimental conditions of the applied DoE model.*

| *LB (min)* | *Conc. (nM)* | *DIC (h)* |
|---|---|---|
| 0 | 0 | 48 |
| 15 | 0 | 48 |
| 0 | 100 | 24 |
| 15 | 100 | 24 |
| 0 | 100 | 48 |
| 15 | 100 | 48 |
| 0 | 100 | 72 |
| 15 | 100 | 72 |
| 0 | 200 | 48 |
| 15 | 200 | 48 |

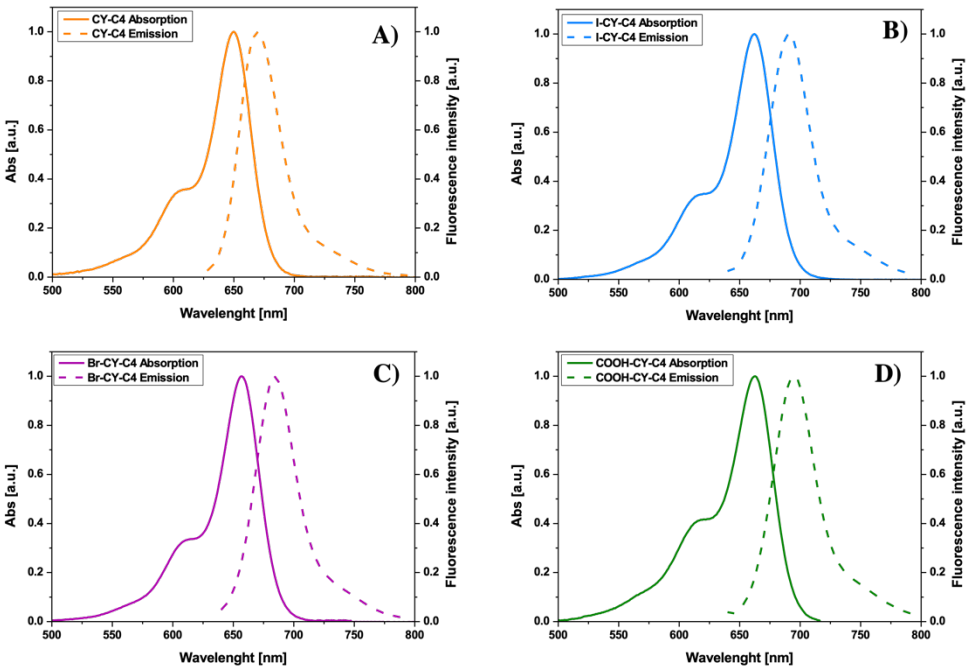


***Figure 2**. Normalized UV–Vis and fluorescence spectra of the synthesized symmetrical cyanines in DMSO.*

***Table 3***. *Selected photophysical properties of symmetrical cyanine dyes in different solvents.*

| | ***CY-C4*** | ***I-CY-C4*** | ***Br-CY-C4*** | ***COOH-CY-C4*** |
|---|---|---|---|---|
| ***Log ε*** | 5.18[1)] | 5.30[1)] | 5.42[1)] | 5.34[1)] |
| ***ε*** ***($M^{-1}$ $cm^{-1}$)*** | $1.52 \times 10^{5}$ [1)] | $2.00 \times 10^{5}$ [1)] | $2.65 \times 10^{5}$ [1)] | $2.19 \times 10^{5}$ [1)] |
| ***$\lambda_{ex}$ max (nm)*** | 650[1)], 644[2)], 646[3)], 642[4)], 641[5)], 655[6)] | 662[1)], 656[2)], 659[3)], 656[4)], not soluble[5)], 670[6)] | 657[1)], 652[2)], 655[3)], 651[4)], not soluble[5)], 665[6)] | 661[1)], 653[2)], 657[3)], 655[4)], 654[5)], 665[6)] |
| ***$\lambda_{em}$ max (nm)*** | 670[1)], 663[2)], 664[3)], 662[4)], 659[5)], 671[6)] | 691[1)], 677[2)], 680[3)], 681[4)], not soluble[5)], 691[6)] | 684[1)], 672[2)], 676[3)], 673[4)], not soluble[5)], 685[6)] | 682[1)], 671[2)], 678[3)], 674[4)], 670[5)], 679[6)] |
| ***QY*** | 0.59[1)] | 0.65[1)] | 0.58[1)] | 0.51[1)] |

[1)] DMSO; [2)] Acetone; [3)] Ethanol; [4)] Methanol; [5)] Water; [6)] DCM

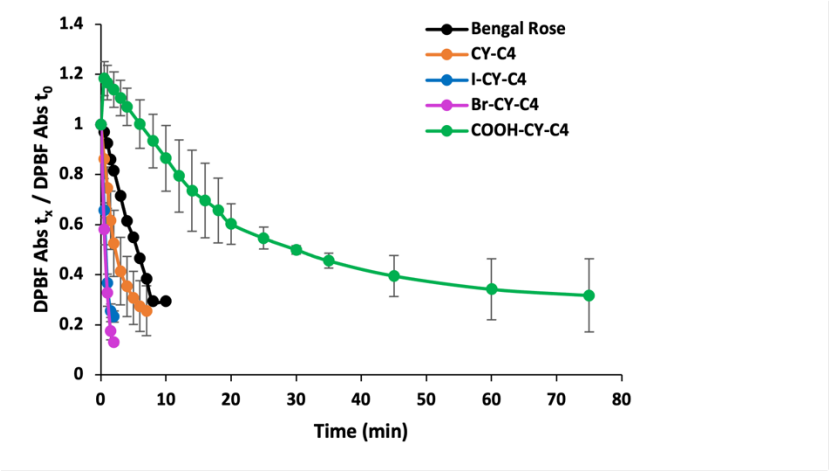


Figure 3. ROS production of all the cyanine dyes compared to the Bengal Rose as standard.

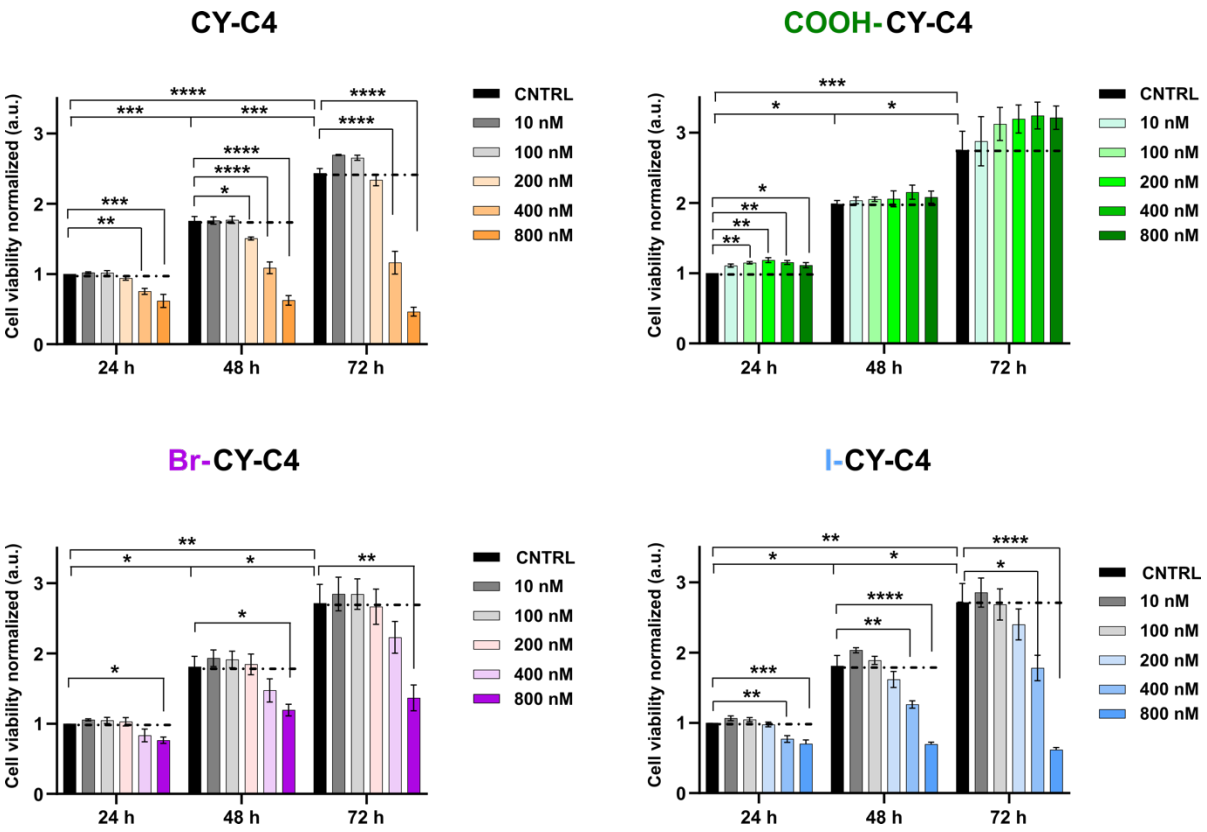


***Figure 4.*** *In vitro cytotoxicity of the cyanines on MCF-7. Cell viability assays on MCF-7 24, 48, and 72 h after treatment with different concentrations of cyanines (CY-C4, COOH-CY-C4, Br-CY-C4, and I-CY-C4). Data are normalized to the CNTRL (MCF-7 untreated) at 24 h and are represented as mean ± SEM. Data refer to the mean of three independent experiments. Statistical significance: *: $p < 0.05$; **: $p < 0.01$; ***: $p < 0.001$; ****: $p < 0.0001$ (Statistical significance versus CNTRL: ordinary one-way ANOVA with post-hoc Dunnett's multiple comparisons test; statistical significance between CNTRL at different time points: ordinary one-way ANOVA with post-hoc Tuckey's multiple comparisons test).*

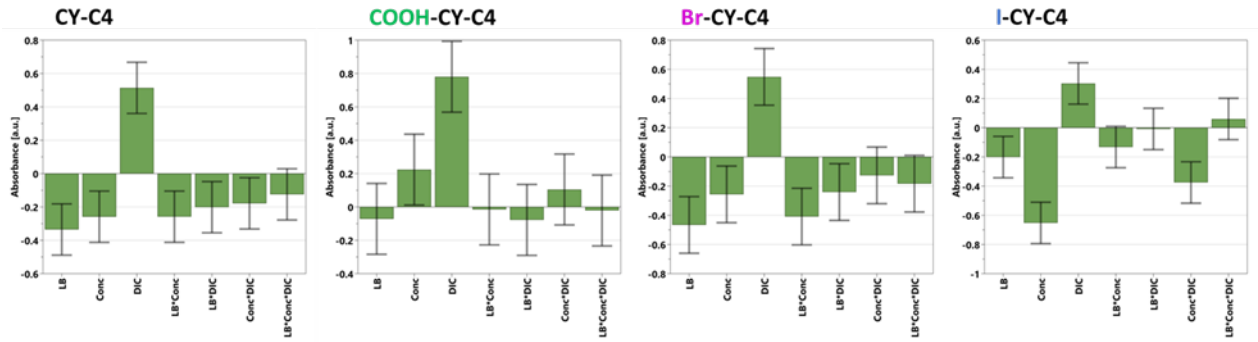


***Figure 5.*** *Cyanine photoactivity models. Coefficient Plots referring to CY-C4, COOH-CY-C4, Br-CY-C4, I-CY-C4 models. The influence of independent factors and their interactions on the cellular response is shown with confidence intervals (error bars) at 95%.*

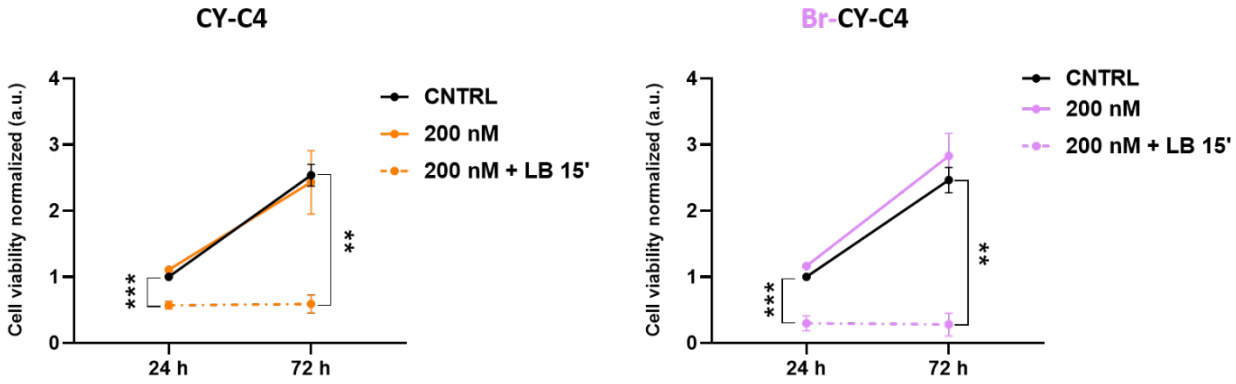


***Figure 6****. Cell viability assays on MCF-7 O/N treated with 200 nM CY kept in the dark (solid lines) or 24 h and 72 h after 15 min light irradiation (640 nm, 7.2 J/cm$^2$ – dashed lines) Data are normalized on the CNTRL at 24 h and represented as mean ± SEM. Data refer to the mean of three independent experiments (n=3). Statistical significance: **: $p < 0.01$; ***: $p < 0.001$ (Statistical significance versus CNTRL: ordinary one-way ANOVA with Dunnett's multiple comparisons post-hoc test).*

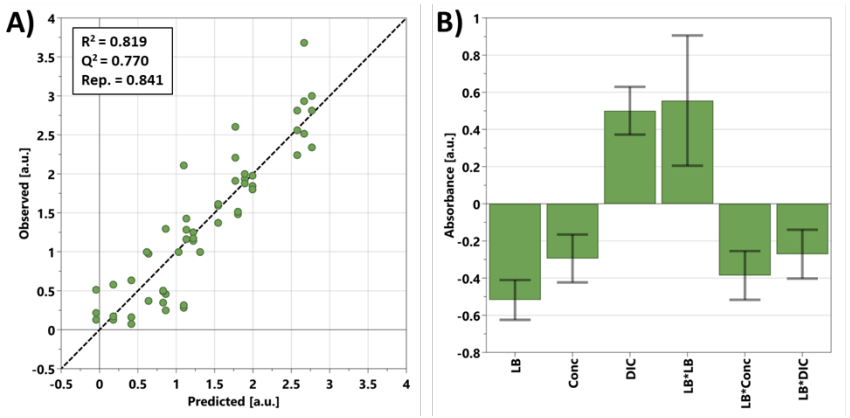


C)

| Coeff. List | Coeff. SC | ±SEM | Conf. int(±) |
|---|---|---|---|
| Constant | 0.83 | 0.17 | 0.33 |
| LB | -0.52 | 0.05 | 0.11 |
| Conc | -0,29 | 0.06 | 0.13 |
| DIC | 0.50 | 0.06 | 0.13 |
| LB*LB | 0.56 | 0.17 | 0.35 |
| LB*Conc | -0.39 | 0.07 | 0.13 |
| LB*DIC | -0.27 | 0.07 | 0.13 |

***Figure 7****. Data analysis on Br-CY-C4 model. A) Observed vs predicted scatter plots (In the box: $R^2$ = explained variation index; $Q^2$ = predict variation index; Rep. = reproducibility data index). B) Coefficient Plot with confidence intervals (error bars) at 95%. C) Table summarizing the value of the coefficients scaled and centred (Coeff. SC), ± SEM, with their confidence interval (95%). Coefficients not significant at the selected confidence level are excluded from the model and not reported.*

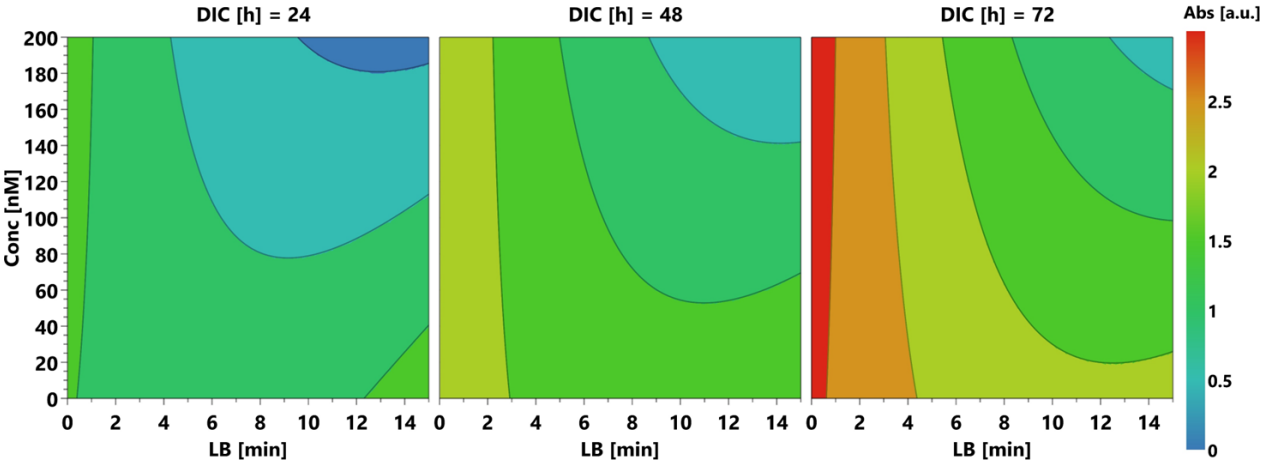


***Figure 8.*** *Isoresponse contour Plot. Calculated cell viability (absorbance) in function of light beam exposure, dye concentration and incubation time.*

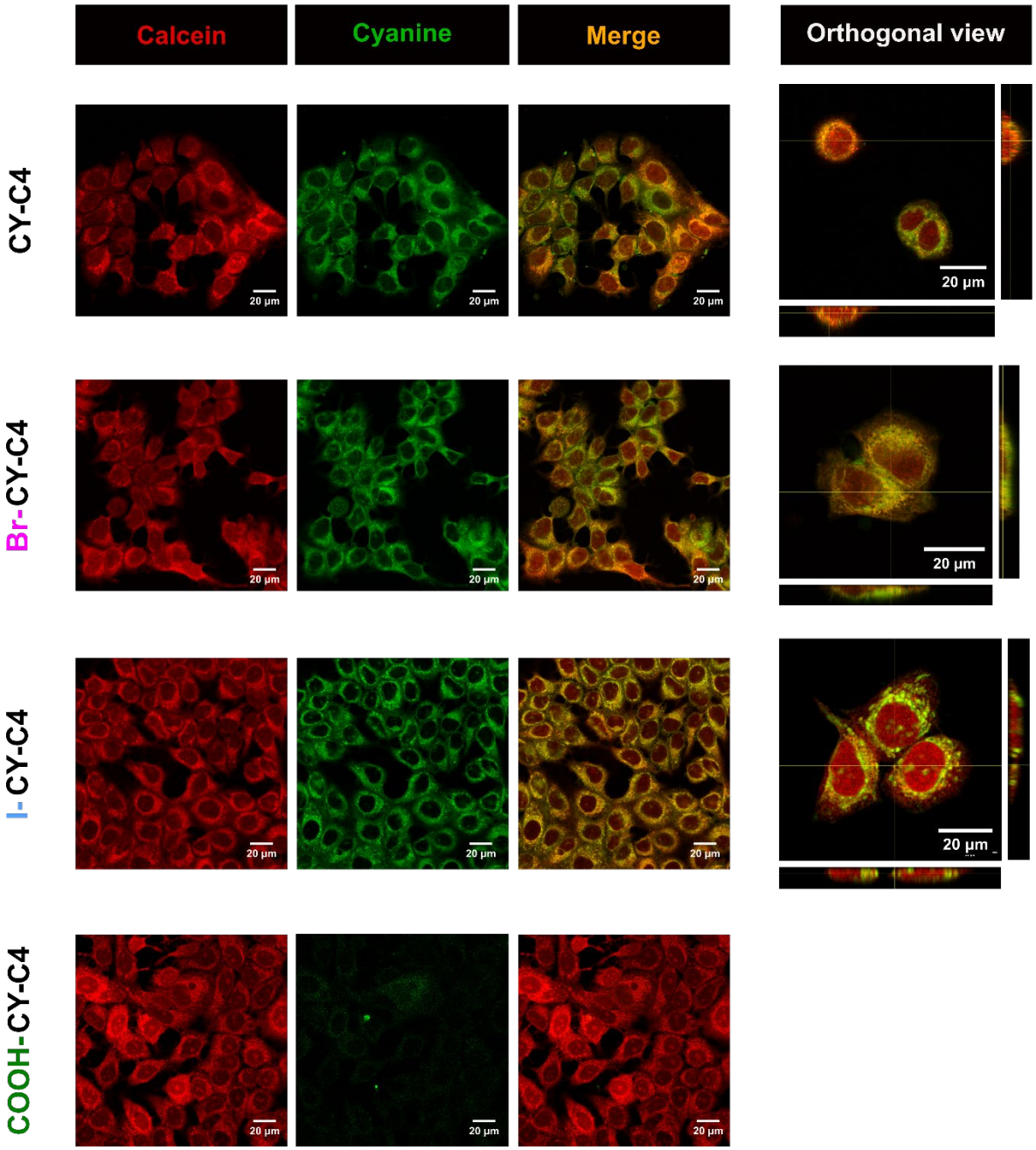


***Figure 9***. *Representative confocal fluorescence images of MCF-7 cells incubated O/N with either CY-C4, Br-CY-C4, I-CY-C4 or COOH-CY-C4 at the same concentration (200 nM). Red signal refers to calcein (λex= 561 nm), green signal refers to cyanines (λex= at 633 nm) and the overlay between the two signals is reported in yellow (merge). For each sample the 3D cellular volume was reconstructed, and orthogonal views are reported. Scale bar: 20 µm.*

# Supplementary Information

# Photosensitizers for photodynamic therapy: Structure-activity analysis of cyanine dyes through Design of Experiments

C. Pontremoli[a,†], G. Chinigò[b,†], S. Galliano[c], M.J. Moran Plata[a,§], D.M. Dereje[a,d], E. Sansone[b], A. Gilardino[b], C. Barolo[a], A. Fiorio Pla[b], S. Visentin[e], N. Barbero[a,*]

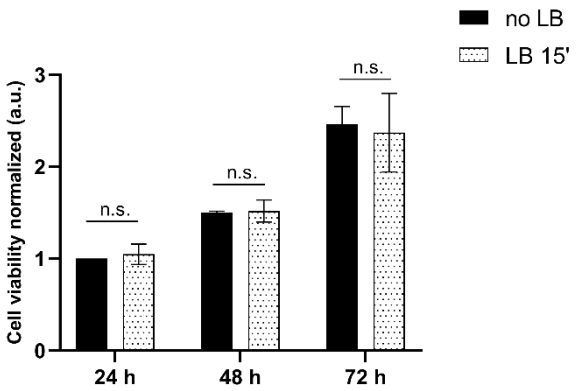


**Figure S1.** ***In vitro*** **phototoxicity of the light beam irradiation**

Cell viability assays on MCF-7 kept in the dark (black columns) or 24 h and 72 h after 15 min LED irradiation (640 nm, 7.2 J/cm$^2$ – white columns). Data are normalized on the CNTRL at 24 h and represented as mean ± SEM. Data refer to 3 independent experiments. Statistical significance versus CNTRL (MCF-7 not irradiated): n.s. not significant (paired Student t-test).

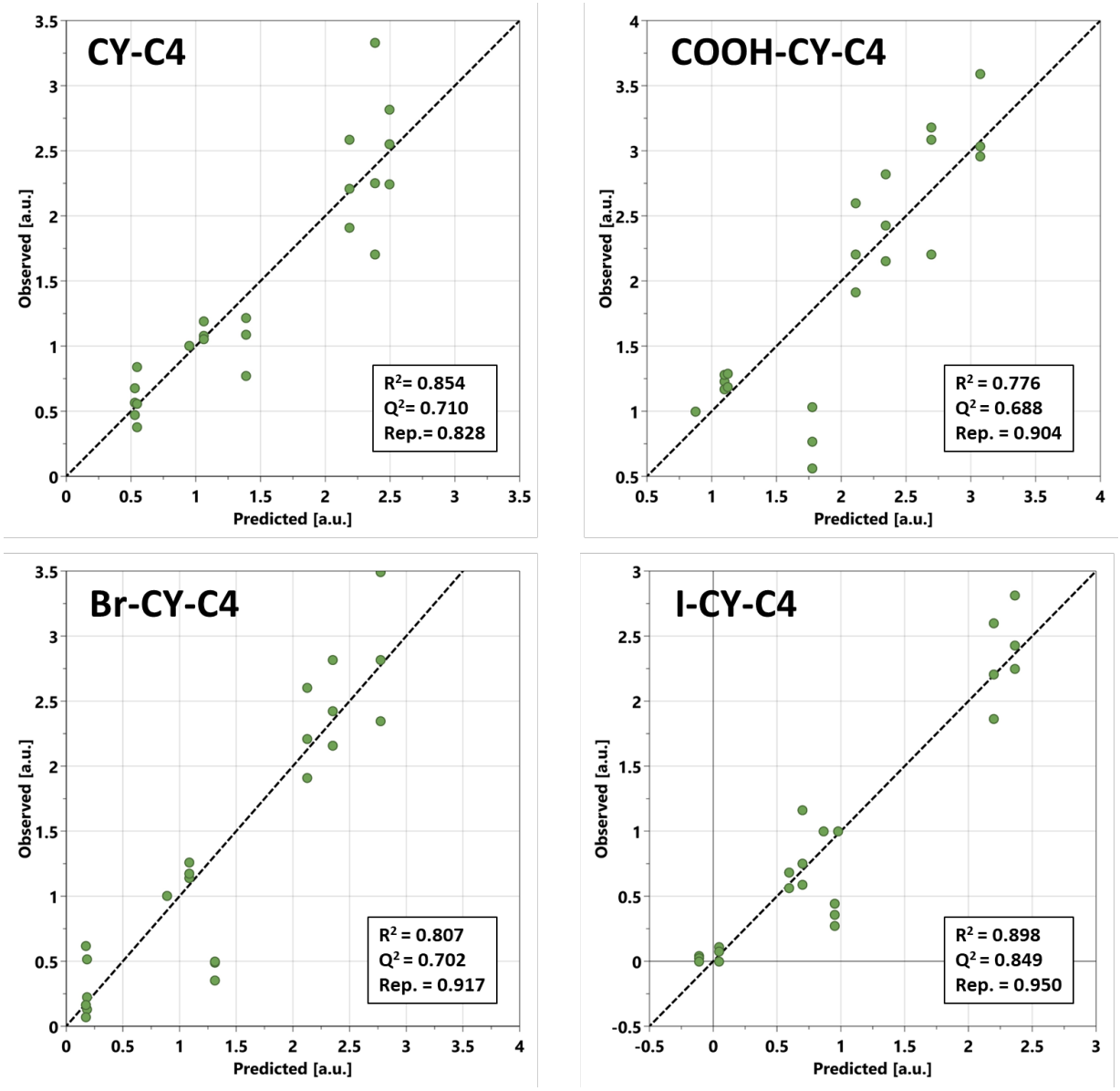


**Figure S2. Model evaluation**

Observed vs predicted scatter plots of the four models. In the box: $R^2$ = explained variation index; $Q^2$ = predict variation index; Rep. = reproducibility data index.

**Table S1. Model coefficients of DoE screening design**

Calculated coefficients of the model function for each cyanine. The value of the coefficients scaled and centred (Coeff. SC) are reported with standard deviation (± SEM) and confidence interval (at 95%). Coefficients not significant at the selected confidence level are reported in red.

**CY-C4**

| Coeff. List | Coeff. SC | ±SEM | Conf. int(±) |
|---|---|---|---|
| Constant | 1.39 | 0.07 | 0.15 |
| LB | -0.34 | 0.07 | 0.15 |
| Conc | -0.26 | 0.07 | 0.15 |
| DIC | 0.51 | 0.07 | 0.15 |
| LB*Conc | -0.26 | 0.07 | 0.15 |
| LB*DIC | -0.20 | 0.07 | 0.15 |
| Conc*DIC | -0.18 | 0.07 | 0.15 |
| LB*Conc*DIC | -0.12 | 0.07 | 0.15 |

**COOH-CY-C4**

| Coeff. List | Coeff. SC | ±SEM | Conf. int(±) |
|---|---|---|---|
| Constant | 1.77 | 0.10 | 0.20 |
| LB | -0.07 | 0.10 | 0.21 |
| Conc | -0.22 | 0.10 | 0.21 |
| DIC | 0.78 | 0.10 | 0.21 |
| LB*Conc | -0.01 | 0.10 | 0.21 |
| LB*DIC | -0.08 | 0.10 | 0.21 |
| Conc*DIC | 0.10 | 0.10 | 0.21 |
| LB*Conc*DIC | -0.02 | 0.10 | 0.21 |

**Br-CY-C4**

| Coeff. List | Coeff. SC | ±SEM | Conf. int(±) |
|---|---|---|---|
| Constant | 1.31 | 0.10 | 0.20 |
| LB | -0.47 | 0.10 | 0.21 |
| Conc | -0.26 | 0.10 | 0.21 |
| DIC | 0.55 | 0.10 | 0.21 |
| LB*Conc | -0.41 | 0.10 | 0.21 |
| LB*DIC | -0.24 | 0.10 | 0.21 |
| Conc*DIC | -0.13 | 0.10 | 0.21 |
| LB*Conc*DIC | -0.18 | 0.10 | 0.21 |

**I-CY-C4**

| Coeff. List | Coeff. SC | ±SEM | Conf. int(±) |
|---|---|---|---|
| Constant | 0.95 | 0.06 | 0.13 |
| LB | -0.20 | 0.07 | 0.14 |
| Conc | -0.65 | 0.07 | 0.14 |
| DIC | 0.30 | 0.07 | 0.14 |
| LB*Conc | -0.13 | 0.07 | 0.14 |
| LB*DIC | -0.01 | 0.07 | 0.14 |
| Conc*DIC | -0.38 | 0.07 | 0.14 |
| LB*Conc*DIC | 0.06 | 0.07 | 0.14 |